Triboelectric Nanogenerator for Harvesting Vibration Energy in Full Space and as Self-Powered Acceleration Sensor

*Hulin Zhang, Ya Yang, Yuanjie Su, Jun Chen, Katherine Adams, Sangmin Lee, Chenguo Hu, and Zhong Lin Wang**

A spherical three-dimensional triboelectric nanogenerator (3D-TENG) with a single electrode is designed, consisting of an outer transparent shell and an inner polyfluoroalkoxy (PFA) ball. Based on the coupling of triboelectric effect and electrostatic effect, the rationally developed 3D-TENG can effectively scavenge ambient vibration energy in full space by working at a hybridization of both the contact-separation mode and the sliding mode, resulting in the electron transfer between the Al electrode and the ground. By systematically investigating the output performance of the device vibrating under different frequencies and along different directions, the TENG can deliver a maximal output voltage of 57 V, a maximal output current of 2.3 μA, and a corresponding output power of 128 μW on a load of 100 MΩ, which can be used to directly drive tens of green light-emitting diodes. Moreover, the TENG is utilized to design the self-powered acceleration sensor with detection sensitivity of 15.56 V g^{-1}. This work opens up many potential applications of single-electrode based TENGs for ambient vibration energy harvesting techniques in full space and the self-powered vibration sensor systems.

1. Introduction

A rapid development of society and the economy has substantially increased energy demands. Much effort has been devoted to harvest ambient energy to meet the worldwide needs. As compared with other ambient environmental energy sources (such as chemical, thermal, or light), mechanical energy is the most abundant in our living environment with considering the availability both in location and time.[1–3] By utilizing the electrostatic, piezoelectric, and electromagnetic effects, various environmental mechanical energy harvesters have been extensively developed.[4–7] Moreover, based on the triboelectric effect coupled with electrostatic induction, triboelectric nanogenerators (TENGs) have been successfully developed to scavenge mechanical energy through either periodic vertical contact-separation or in-plane sliding/rotating.[8–12] However, all of the reported mechanical/vibration energy harvesters are usually capable of working along only one direction, resulting in that the energy from other directions was wasted. It is necessary to develop new techniques to scavenge vibration energy from multiple directions, even full space, for realizing the maximum energy harvesting.

Usually, the acceleration sensors are based on force sensing mechanisms, including piezoresistive or differential capacitance, which have a wide variety of applications for industrial engineering, biology and navigation.[13–16] An external power source is indispensable to drive these sensors. Self-powered nanotechnology is based on utilizing energy harvesters instead of external power sources or batteries to drive the sensors.[17–22] TENGs have been reported as self-powered sensors for detecting change of magnetic field, mercury ions, and glucose.[20–23]

In this paper, we demonstrated a newly designed 3D-TENG that consists of one inner PFA ball and an outer transparent sphere. One Al sheet was adhered to the inner surface of the outer sphere and was used as the electrode. The fabricated TENG can scavenge the vibration energy in full space by working at a hybridization of both the contact-separation mode and the sliding mode. The electricity generated by shaking the spherical TENG can directly light up 35 commercial green light-emitting diodes (LEDs). Furthermore, we demonstrated that the fabricated TENG can be utilized as an active self-powered sensor to detect the vibration acceleration, where the sensitivity is 15.56 V g^{-1}. This work will push the development and expand potential applications of single-electrode based TENGs for scavenging different forms of vibration energy and as self-powered sensor systems.

H. L. Zhang, Dr. Y. Yang, Y. J. Su, J. Chen, K. Adams, Dr. Sangmin Lee, Prof. Z. L. Wang
School of Materials Science and Engineering
Georgia Institute of Technology
Atlanta, Georgia, 30332–0245, USA
E-mail: zhong.wang@mse.gatech.edu
H. L. Zhang, Dr. C. G. Hu
Department of Applied Physics
Chongqing University
Chongqing, 400044, China
Prof. Z. L. Wang
Beijing Institute of Nanoenergy and Nanosystems
Chinese Academy of Sciences, Beijing, China

DOI: 10.1002/adfm.201302453

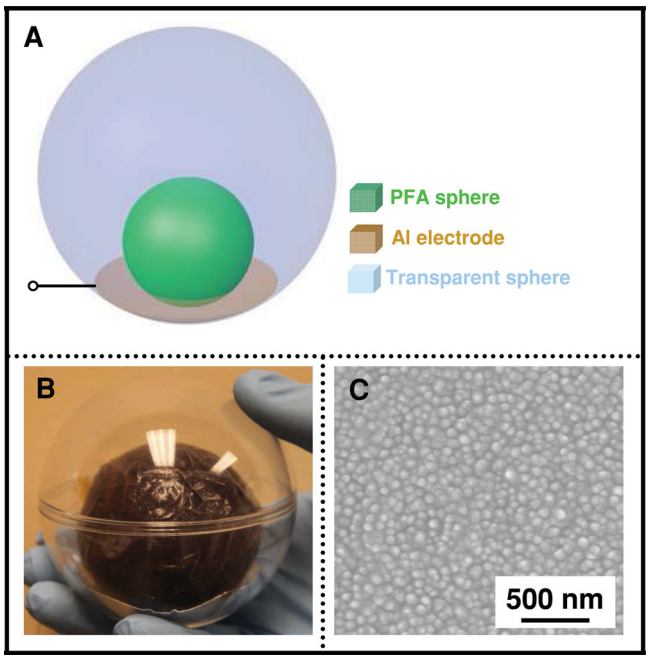

Figure 1. Device structure of a spherical TENG. A) The schematic diagram. B) Photograph of a fabricated TENG. C) SEM image of PFA surface with etched nanoparticle structure.

2. Results and Discussion

As sketched in **Figure 1**A, the spherical TENG consists of two spheres. An ordinary rubber ball was coated with etched PFA film to form a PFA ball, where the PFA film acts as a triboelectric polymer. The inner PFA ball can slide and bounce freely inside the transparent shell. A thin Al foil was adhered to the inner surface of the outer sphere, acting as both the triboelectric layer and the electrode. Figure 1B displays a corresponding photograph of TENG. In order to enhance the performance of the TENG,[24] the PFA film was dry-etched using ICP to create the nanoparticle-like structures on the surface. Figure 1C illustrates a SEM image of the etched PFA surface, revealing that the surface is uniformly covered with a nanoparticle structure and the diameters are smaller than 100 nm.

The working mechanism of the fabricated 3D-TENG is schematically plotted in **Figure 2**. There are two different operating principles when the TENG vibrates along different directions. When vibrating vertically, the process of generating electricity is depicted in Figure 2A. At the original state (Figure 2Aa), when the PFA ball stays at the bottom due to its gravity and contacts with the Al electrode, the surface charges were generated between the PFA ball and the Al electrode due to the triboelectric effect. Since Al is more triboelectrically positive than PFA according to the triboelectric series,[25] the PFA and the Al electrode have the negative and positive charges, respectively. Due to the insulation property of the PFA ball, the generated negative triboelectric charges can be preserved on its surface for an extended period of time. At this moment, triboelectric charges with opposite polarities are fully balanced out with little electric potential drop across the Al electrode and PFA, making no electric output in the external circuit. However, once the PFA

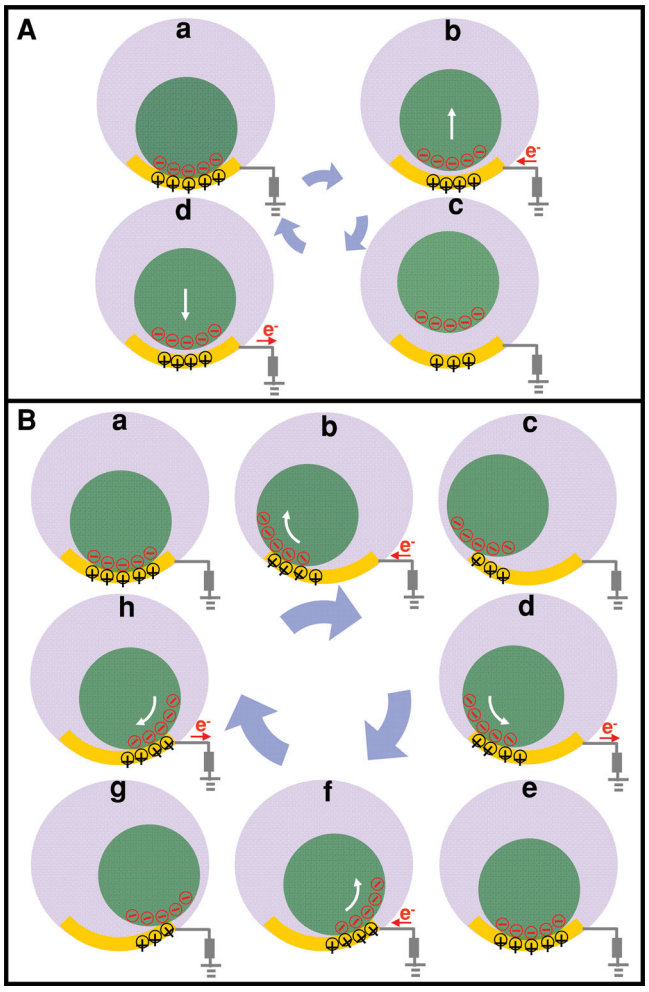

Figure 2. Two typical working mechanisms of the spherical TENG with single electrode that illustrates the electricity generation process in a full cycle of the TENG. A) Working mechanism of the TENG vibrating along the vertical direction. B) Working mechanism of the TENG vibrating along the horizontal direction.

ball bounces up and separates from the Al electrode, the equilibration of electric field is changed, inducing a higher potential at the Al electrode (Figure 2Ab). As a result, electrons can flow through an external load from the ground to the conductive Al electrode, which is due to the edge electric field leakage from the finite sized Al electrode and PFA ball. The flow of induced electrons can last until a new electrical equilibrium is established (Figure 2Ac) as the PFA ball continues to rise up. Subsequently, the PFA ball drops back to its original state, driving electron flow back into the ground (Figure 2Ad). The contact-separation process is the working mode for the TENG vibrating along the vertical direction. The typical working diagram for the TENG vibrating horizontally is displayed in Figure 2B. Originally, the PFA ball stays at the bottom, resulting in that the PFA has the negative charges while the Al electrode has the positive charges (Figure 2Ba). When the PFA ball slides away from the Al electrode, triboelectric charges on the mismatched areas cannot be compensated and will generate an electrical inequilibrium. The electrical potential difference

at the interface can force electrons to flow from the ground to the Al electrode because of the edge electric field leakage (Figure 2Bb). Then, the PFA ball is separated from the Al electrode to create a new electrical equilibrium, resulting in no output current/voltage, as illustrated in Figure 2Bc. Consequently, the PFA ball slides back and is in contact with the Al electrode (Figure 2Bd). To establish a new electrical equilibrium, the electrons are driven back to the ground. Similarly, when sliding on the reversed side of the transparent ball, the electrons can also flow through the external load. The sketched diagrams are illustrated in Figure 2Be–h. The cycle of sliding away and back generates electricity from vibration along the horizontal direction. Moreover, when the TENG vibrates obliquely, the electricity generation comes from a combination of contact-separation and sliding mode.

To demonstrate the availability of the spherical TENG that can scavenge the vibration energy from full space, the output performance of TENG was systematically investigated. **Figure 3** depicts the output voltage and current signals of the TENG vibrating along different coordinate axis, where the corresponding schematic diagrams are displayed in Figures 3A,D,G, respectively. The output voltage and current at different vibration frequencies, ranging from 2 Hz to 100 Hz, were recorded. Under the vibrating frequency of 20 Hz in the vertical direction (±*Z* axis), the maximum output voltage, current and power are 57 V, 2.3 μA and 128 μW, respectively. As illustrated in Figure 3B, real-time curves of maximum output voltage and current reveal that the signals are uniform and stable. Figure 3C shows the frequency dependence on voltage, current and power of the TENG when vibrating along ±*Z* axis, indicating that the output performance of the device can increase at the low frequencies (<20 Hz) and then drop with successive increase of frequency. This is because the vibrational system reaches its natural resonance frequency at around 20 Hz. At the at resonance state, the vibration amplitude of inner ball and outer sphere can be maximal, leading to the inner ball separating farthest from the Al electrode and colliding most forcefully with the Al electrode which is adhered to the inner surface of the outer sphere. As a result, the output performance of the TENG can be up to the maximum at around 20 Hz due to the output performance positively correlated with separation distance and collision force according to the previous literature.[24] Moreover, the output performances of the TENG vibrating along the ±*X* axis and the ±*Y* axis are given in Figures 3D–F and Figures 3G–I, respectively. These data show similar trends with the TENG vibrating along ±*Z* axis.

To further investigate the performance of the spherical TENG, the output performances of the TENG vibrating at different angles in the *Y*–*Z* plane were measured. The corresponding schematic diagrams and relationships between voltage/current/power and frequency are illustrated in **Figure 4**. As illustrated in Figure 4A, the output performance of the TENG decreases after it increases at the lower frequencies (<22 Hz, resonance frequency) when vibrating at −30 degrees to the *Y*-axis. While the TENG vibrated at −60 degrees, +30 degrees, and +60 degrees to the *Y* axis, the similar results can be observed, as displayed in Figures 4B–D, respectively. To present the stable output performance of the device, the real-time curves of maximum output voltage and current, with the TENG vibrating at different angles, are shown in Figures S1–S4 (Supporting Information), respectively, exhibiting an excellent and desirable performance.

To depict the output performance distribution of the spherical TENG vibrating along different directions, numerical simulations of output performances are performed, as shown in **Figure 5**A (voltage), 5B (current), and 5C (power). These simulation results reveal that the maximum output performance was achieved along the vertical direction. As the vibrating direction of the TENG gradually approaches horizontal, the output voltage/current/power decreases, which is because that the PFA ball yields maximum vertical separation and effective contact with the Al electrode due to gravity along the vertical direction. Once the angle of vibration is not vertical, the PFA ball gets smaller separation and contact with the Al electrode due to the PFA ball's slanting bounce. Meanwhile, the sliding away-back mode is introduced and gradually dominates the triboelectric process with increasing angle of inclination. Nevertheless, the output performance is desirable even when the TENG vibrates along a horizontal line. In other words, the vibrational energy from all directions, or in full space, can be efficiently converted into electricity by the spherical 3D-TENG.

A demonstration of the spherical TENG as a direct power source for driving LEDs is presented in Figure 5D–F. An electric circuit diagram of inner and outer LEDs connected to the TENG is displayed in Figure S5, Supporting Information. Figure 5D shows a photograph of the LEDs when there was no vibration. When the TENG vibrates along the vertical direction at a frequency of 20 Hz, the inner LEDs were lighted up from the forward current while the outer LEDs were lighted up from the reversed current flow, as illustrated in Figures 5E,F, respectively. The result is completely consistent with the alternating current (AC) output of the 3D-TENG.

To demonstrate the potential applications of the spherical TENG further, the TENG was utilized as an active self-powered acceleration sensor. **Figure 6** shows the performance of a TENG based acceleration sensor. The output voltages of the sensor at specific acceleration are enumerated in Figures 6A–E and Figure S6, Supporting Information. It can be seen clearly that all of the output voltage signals are uniform and stable. The relationship between output voltage and acceleration is plotted in Figure 6F, revealing a clear linear relationship by fitting the data, which is beneficial for practical applications of the sensors. The detection sensitivity of the acceleration was calculated to be about 15.56 V g^{-1}.

3. Conclusions

In summary, we have demonstrated a newly designed spherical 3D-TENG for harvesting vibration energy in full space and as a self-powered acceleration sensor. The relationship between the output performance of the TENG and the working frequency/directions was systematically investigated. By working at a hybridization of both the contact-separation mode and the sliding mode, the fabricated 3D-TENG can effectively scavenge vibration energy from all directions, and deliver a maximum voltage of 57 V, a maximum current of 2.3 μA, and a maximum power of 128 μW. Due to a linear relationship between the

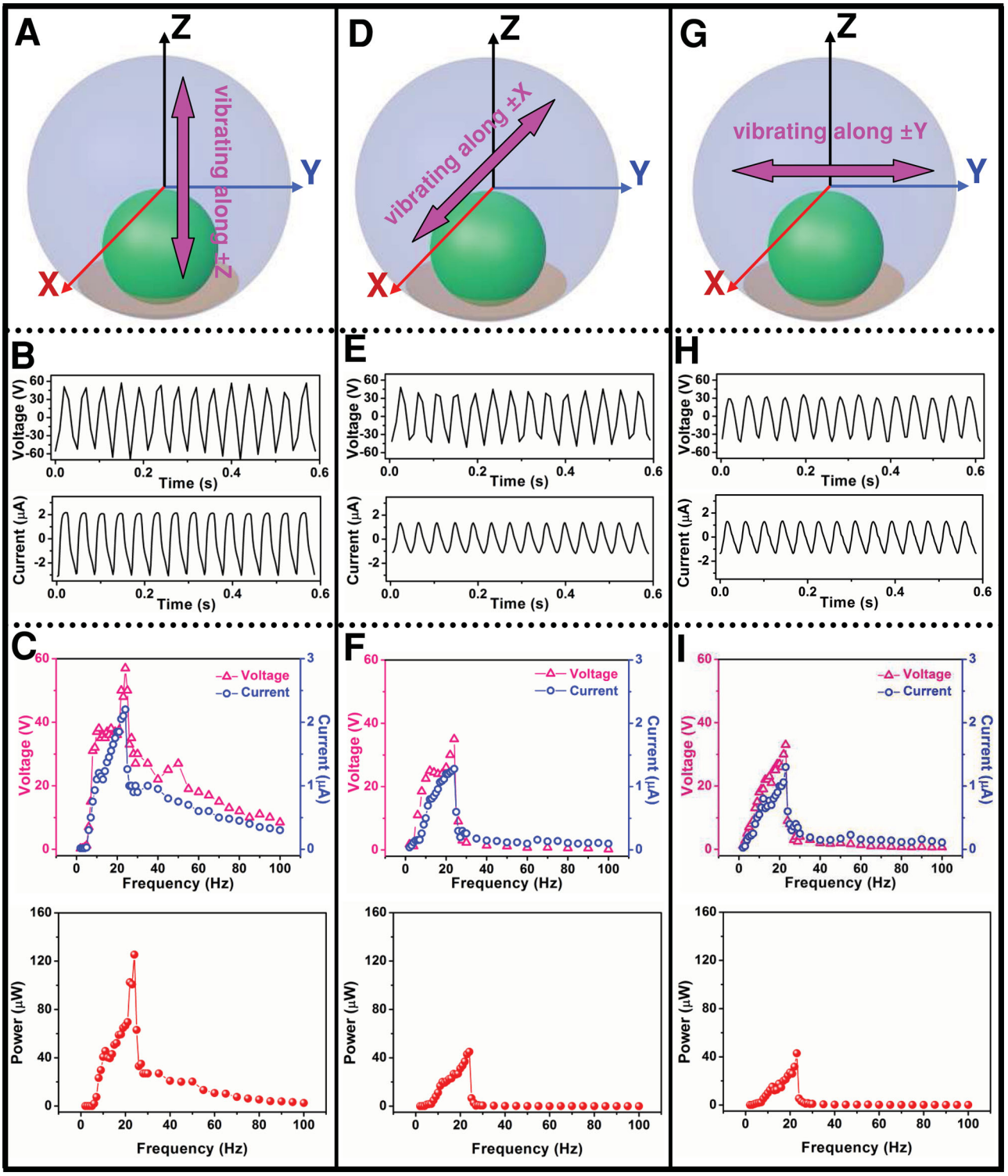

Figure 3. Output performance of the TENG vibrating along the three coordinate axes. A) Schematic diagram, B) maximal output voltage/current, and C) summarized relationship between the voltage/current/power and vibration frequency vibrating along ±*Z*. D) Schematic diagram, E) maximal output voltage/current, and F) summarized relationship between the voltage/current/power and vibration frequency vibrating along ±*X*. G) Schematic diagram, H) maximal output voltage/current, and I) the summarized relationship between the voltage/current/power and vibration frequency vibrating along ±*Y*.

output voltage and acceleration, the TENG has been utilized as an active self-powered acceleration sensor with detection sensitivity of about 15.56 V g^{-1}. The fabricated 3D-TENGs have the potential applications in the vibration energy harvesting from multiple or time-variant directions and the self-powered vibration sensor systems.

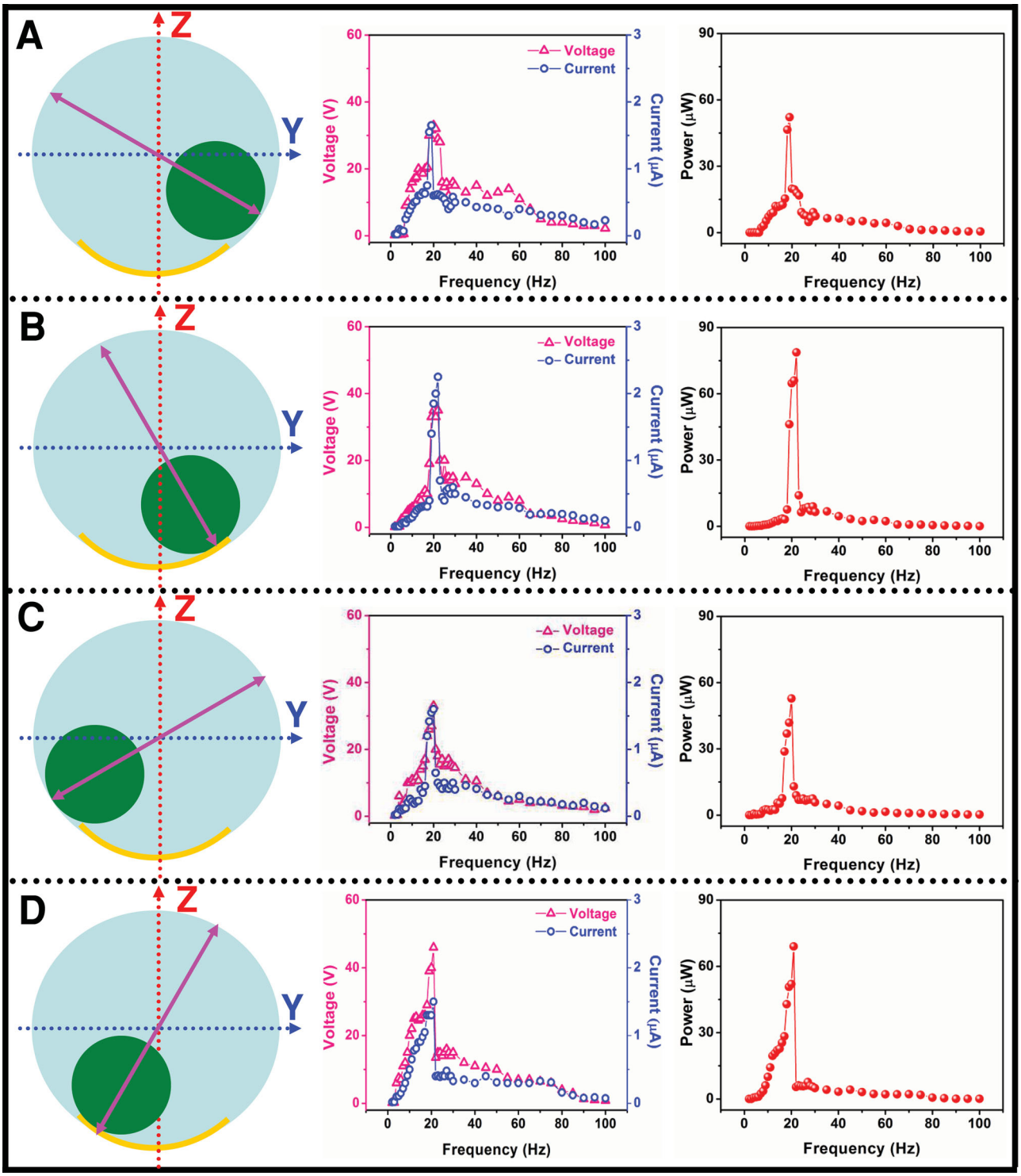

Figure 4. Output performance of the TENG vibrating along the different oblique angle in *Y–Z* plane. A) Schematic diagram and summarized relationship between the voltage/current/power and frequency vibrating with –30 degrees to the Y axis. B) Schematic diagram and summarized relationship between the voltage/current/power and frequency vibrating with –60 degrees to the *Y* axis. C) Schematic diagram and summarized relationship between the voltage/current/power and frequency vibrating with +30 degrees to the Y axis. D) Schematic diagram and summarized relationship between the voltage/current/power and frequency vibrating with +60 degrees to the *Y* axis.

4. Experimental Section

Nanoparticle-Based Surface Modification of PFA Film: A PFA film with a thickness of 50 μm was cleaned with isopropyl alcohol and deionized water, then blown dry with nitrogen gas. Subsequently, a thin Au film, as the mask for etching the PFA surface, was deposited on the PFA surface using a DC sputter. Then, inductively coupled plasma (ICP) reactive ion etching was utilized to produce nanoparticle-based modification

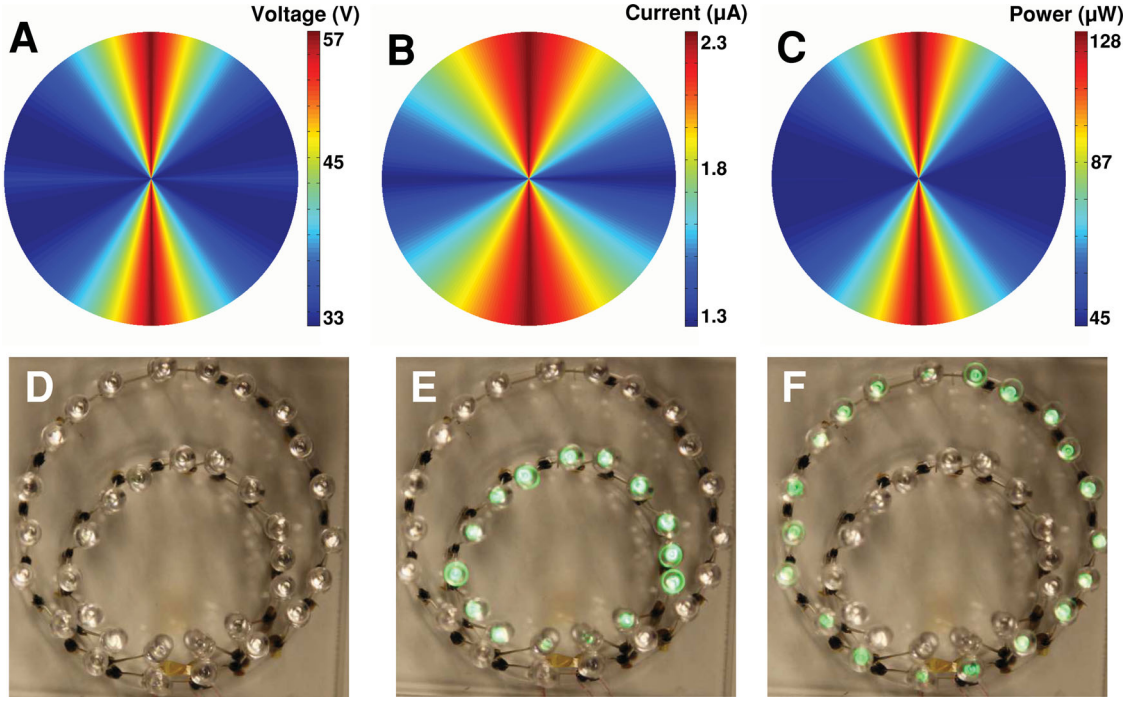

Figure 5. Simulation of maximal output performance of the TENG vibrating along different directions. A–C) Distribution of maximal output voltage/current/power of the TENG. Demonstration of the TENG as a direct power source for driving LEDs. D) Photograph of the original LEDs. E) Photograph of the inner LEDs lighted by the forward current. F) Photograph of the outer LEDs lighted by the reversed current flow.

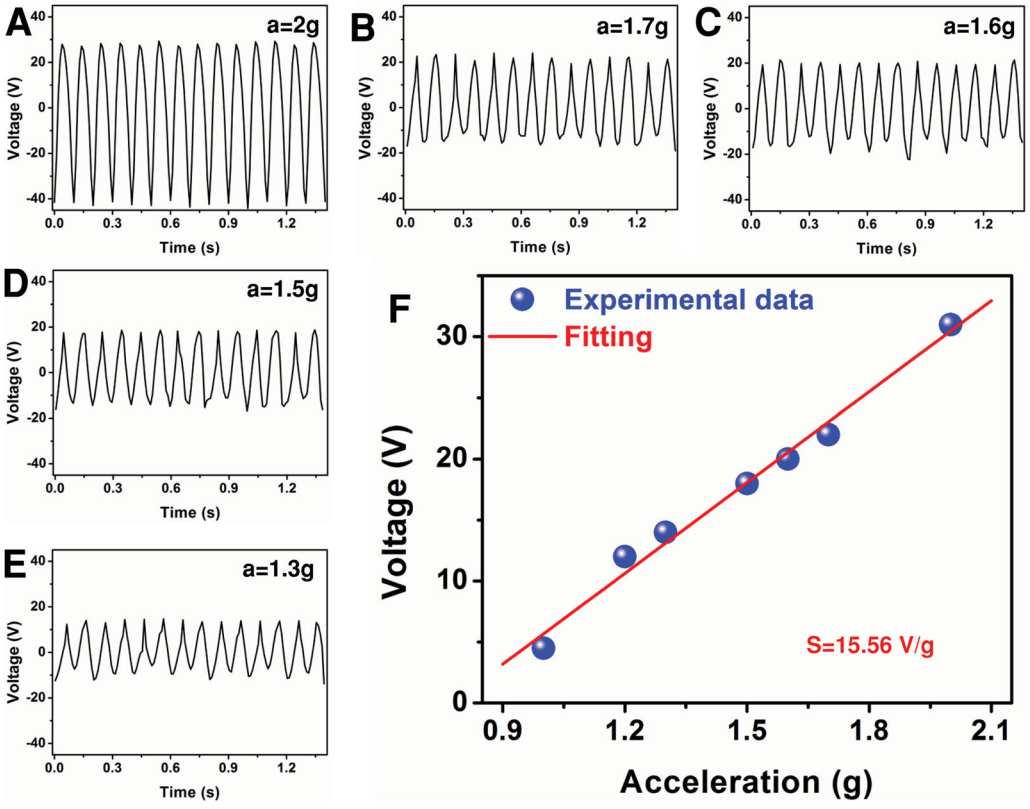

Figure 6. Performance of acceleration sensor based on TENG. A–E) Output voltage of the sensor subjected with certain acceleration. F) Dependence of the output voltage on the acceleration.

on the surface of the PFA film. Specifically, Ar, O_2, and CF_4 gases were introduced into the ICP chamber with flow rates of 15, 10, and 30 sccm, respectively. One power source of 400 W was used to generate a large density of plasma, while another 100 W was used to accelerate the plasma ions. The PFA thin film was etched for 10 s in order to produce nanoparticle-like structures on the surface.

Fabrication of a Spherical TENG: First, a smaller rubber ball was fully wrapped with etched PFA film, to form a PFA ball. Then Al foil, as the electrode, with an area of 12.6 cm^2 was adhered to the inner surface of a larger transparent sphere. Finally, the transparent sphere, consisted of two hemispheres and bought from the local Wal-Mart without any modifications, was sealed to shut with the PFA ball inside.

Electric Output Measurement: While measuring the electrical output, the spherical TENG was fixed on the electrodynamic shaker (Labworks ET-139), which was driven by an amplified sinusoidal wave from a function generator (Labworks SC-121) and an amplifier (Labworks Pa-151). The Al electrode remained at the bottom of the inner surface of the outer sphere when the shaker was tilted at different angles. The output voltage of the TENG was measured by a Keithley 6514 system electrometer and the output current was recorded by a low noise current amplifier (Stanford Research System SR570) under a loading resistance of 100 MΩ.

When demonstrating the potential applications of the spherical TENG as an active self-powered acceleration sensor, the TENG was still fixed on the electrodynamic shaker and kept vibrating in the vertical direction (±*Z* axis). The shaker can vibrate with different accelerations under the control of the function generator, resulting in the TENG vibrating with different certain accelerations. The corresponding output voltages were recorded when the TENG vibrating with different accelerations at the certain frequency of 10 Hz.

Supporting Information

Supporting Information is available from the Wiley Online Library or from the author.

Acknowledgements

H.L.Z and Y.Y. contributed equally to this work. This work was supported by U.S. Department of Energy, Office of Basic Energy Sciences (DE-FG02–07ER46394), ARO MURI, NSF, MANA, National Institute For Materials, Japan, a joint project with Sungkyunkwan University, Korea. H.L.Z. and C.G.H. acknowledge the support of NSFCQ (cstc2012jjB0006), SRFDP (20110191110034), Project (WLYJSBJRCTD201101) of the Innovative Talent Funds for 985 Project of Chongqing University. H.L.Z. also would like to acknowledge the fellowship from the China Scholarship Council (CSC).

Received: July 21, 2013
Revised: August 30, 2013
Published online: October 8, 2013

[1] Z. L. Wang, J. H. Song, *Science* **2006**, *312*, 242.
[2] Y. Yang, W. Guo, K. C. Pradel, G. Zhu, Y. Zhou, Y. Zhang, Y. Hu, L. Lin, Z. L. Wang, *Nano Lett.* **2012**, *12*, 2833.
[3] Y. Yang, H. L. Zhang, J. Chen, S. Lee, T.-C. Hou, Z. L. Wang, *Energ. Environ. Sci.* **2013**, *6*, 1744.
[4] P. Miao, P. D. Mitcheson, A. S. Holmes, E. M. Yeatman, T. C. Green, B. H. Stark, *Microsyst. Technol.* **2006**, *12*, 1079.
[5] C. E. Chang, V. H. Tran, J. B. Wang, Y. K. Fuh, L. W. Lin, *Nano Lett.* **2010**, *10*, 726.
[6] X. D. Wang, J. H. Song, J. Liu, Z. L. Wang, *Science* **2007**, *316*, 102.
[7] S. P. Beeby, R. N. Torah, M. J. Tudor, P. Glynne-Jones, T. O'Donnell, C. R. Saha, S. Roy, *J. Micromech. Microeng.* **2007**, *17*, 1257.
[8] F. R. Fan, Z. Q. Tian, Z. L. Wang, *Nano Energy* **2012**, *1*, 328.
[9] F. R. Fan, L. Lin, G. Zhu, W. Z. Wu, R. Zhang, Z. L. Wang, *Nano Lett.* **2012**, *12*, 3109.
[10] S. H. Wang, L. Lin, Z. L. Wang, *Nano Lett.* **2012**, *12*, 6339.
[11] S. H. Wang, L. Lin, Y. N. Xie, Q. S. Jing, S. M. Niu, Z. L. Wang, *Nano Lett.* **2013**, *13*, 2226.
[12] L. Lin, S. H. Wang, Y. N. Xie, Q. S. Jing, S. M. Niu, Y. F. Hu, Z. L. Wang, *Nano Lett.* **2013**, *13*, 2916.
[13] A. Kazama, T. Aono, R. Okada, *J. Microelectromech. Syst.* **2013**, *22*, 386.
[14] R. Kuells, S. Nau, M. Salk, K. Thoma, *Sens. Actuator A-Phys.* **2012**, *182*, 41.
[15] M. Benmessaoud, MM. Nasreddine, *Microsyst. Technol.* **2013**, *19*, 713.
[16] W. Tian, S. C. Wu, Z. B. Zhou, S. B. Qu, Y. Z. Bai, J. Luo, *Rev. Sci. Instrum.* **2012**, *83*, 095002.
[17] Y. Yang, Y. S. Zhou, J. M. Wu, Z. L. Wang, *ACS Nano* **2012**, *6*, 8456.
[18] Q. Yang, Y. Liu, Z. T. Li, Z. Y. Yang, X. Wang, Z. L. Wang, *Angew. Chem. Int. Ed.* **2012**, *51*, 6443.
[19] Z. L. Wang, *Adv. Mater.* **2011**, *24*, 280.
[20] Y. Yang, L. Lin, Y. Zhang, Q. S. Jing, T.-C. Hou, Z. L. Wang, *ACS Nano* **2012**, *6*, 10378.
[21] Z. H. Lin, G. Zhu, Y. S. Zhou, Y. Yang, P. Bai, J. Chen, Z. L. Wang, *Angew. Chem. Int. Ed.* **2013**, *52*, 1.
[22] H. L. Zhang, Y. Yang, T.-C. Hou, Y. J. Su, C. G. Hu, Z. L. Wang, *Nano Energy* **2013**, DOI: 10. 1016/j. nanoen.2013.03.024.
[23] Y. Yang, H. L. Zhang, R. Y. Liu, X. N. Wen, T.-C. Hou, Z. L. Wang, *Adv. Energy Mater.* **2013**, DOI: 10.1002/aenm.201300376.
[24] G. Zhu, C. F. Pan, W. X. Guo, C. Y. Chen, Y. S. Zhou, R. M. Yu, Z. L. Wang, *Nano Lett.* **2012**, *12*, 4960.
[25] E. Nemeth, V. Albrecht, G. Schubert, F. Simon, *J. Electrostat.* **2003**, *58*, 3.